

1 **Polycomb Repressive Complex 2-controlled Essrg regulates intestinal Microfold**
2 **cell differentiation**

3 Joel Johnson George¹, Mikko Oittinen¹, Laura Martin-Diaz¹, Veronika Zapilko¹, Sharif Iqbal^{2,3},
4 Terhi Rintakangas¹, Fábio Tadeu Arrojo Martins¹, Henri Niskanen⁵, Pekka Katajisto^{2,3,4}, Minna
5 Kaikkonen⁵, Keijo Viiri^{1*}

6 ¹Faculty of Medicine and Health Technology, Tampere University Hospital, Tampere University
7 Tampere, Finland.

8 ²Institute of Biotechnology, HiLIFE, University of Helsinki, Helsinki, Finland.

9 ³Faculty of Biological and Environmental Sciences, University of Helsinki, Finland.

10 ⁴Department of Cell and Molecular Biology, Karolinska Institutet, Stockholm, Sweden.

11 ⁵Department of Biotechnology and Molecular Medicine, A.I. Virtanen Institute for Molecular
12 Sciences, University of Eastern Finland, Kuopio, Finland.

13 *Address correspondence to: Keijo Viiri, PhD, Faculty of Medicine and Health Technology,
14 Tampere University and Tampere University Hospital, Arvo Ylpön katu 34, Tampere, FIN-33520,
15 Finland. e-mail: keijo.viiri@tuni.fi.

16

17

18

19

20

21

22 **Abstract**

23 Microfold cells (M cells) are immunosurveillance epithelial cells located in the Peyer's patches in the
24 intestine responsible for monitoring and transcytosis of antigens, microorganisms and pathogens.
25 Many transcription factors, e.g., Spi-B and Sox8, necessary to M cell differentiation have been
26 described but the exhaustive set of factors sufficient for differentiation and development of a mature
27 M cell remains elusive. Moreover, the role of polycomb repressive complex 2 (PRC2) as an epigenetic
28 regulator of M cell development has not yet been interrogated. Here, we show that PRC2 regulates a
29 significant set of genes during the M cell differentiation including many transcription factors.
30 Estrogen related receptor gamma (Esrrg) is a novel M cell specific transcription factor acting on a
31 RankL-Rank induced NF-kB pathway, upstream of Sox8 and necessary but not sufficient for a mature
32 M cell marker Gp2 expression. To conclude, with the aid of PRC2 target survey we identified the list
33 of developmental genes specifically implicated in M cell development and Esrrg as a necessary factor
34 for Sox8-mediated M cell differentiation.

35 **Keywords:** PRC2/Microfold cells/Esrrg/RankL/Gut Immunity

36

37

38

39

40

41

42

43

44 **Introduction**

45 The Gut-associated lymphoid tissue (GALT) is involved in immune surveillance of antigens,
46 microorganisms and foreign pathogens that constantly thrive in the mucosal surface of the intestinal
47 tract. The GALT is the immune initiation site against mucosal antigens and houses specialized gut
48 immune epithelial cells known as M cells or Microfold cells, these cells envelop the luminal surface
49 of GALT also known Peyer's patches (PPs). (Mabbott et al., 2013; Neutra et al., 1996; Owen, 1999).
50 The principal role of the M cells is the uptake and transcytosis of luminal antigens into the GALT as
51 they have a high phagocytic and transcytosis capacity, which is responsible for the rapid transport of
52 bacterial antigens to antigen-presenting immature dendritic cells (Neutra et al., 2001; Rios et al.,
53 2016). Subsequently, these dendritic cells undergo maturation and activate antigen specific naive T
54 cells, that support B cell activation, resulting ultimately in the generation of IgA-producing plasma
55 cells (Kraehenbuhl & Neutra, 2000). It has been shown previously that the absence of M cells or their
56 antigen uptake receptor glycoprotein 2 (Gp2) mitigates the mucosal immune responses by T cells in
57 mice infected with *Salmonella enterica* serovar Typhimurium. This is predominantly due to lack of
58 bacterial transcytosis by the mature GP2 receptor into the GALT (Kanaya et al., 2012; Kimura et al.,
59 2019). Correspondingly, perturbances in transcytosis of *Yersinia enterocolitica* in PPs were observed
60 in Aif1 mutant mice (Kishikawa et al., 2017). Recently, it was shown that M cells self-regulate their
61 differentiation by expressing osteoprotegerin (OPG), a soluble inhibitor of RANKL, which
62 suppresses the differentiation of adjacent FAE cells into M cells. This self-regulatory machinery of
63 M cell density is necessary as *Opg*^{-/-} mice were highly susceptible to mucosal infection by pathogenic
64 bacteria because of the augmentation of bacterial translocation via M cells (Kimura et al., 2020).
65 Overall, defects in M cell-dependent antigen uptake led to a decrease in production of antigen-specific
66 secretory IgA (S-IgA) in the gut (Hase et al., 2009; Kishikawa et al., 2017; Rios et al., 2016).
67 M cell differentiation of cycling intestinal crypt cells that express Lgr5 and RANK receptors is
68 induced by the Receptor activator of nuclear factor-κB ligand (RankL). RankL is secreted by stromal

69 cells also known as M-cell inducer cells (MCi cells) or immune cells in the sub epithelial dome (SED)
70 (Mabbott et al., 2013; Nagashima et al., 2017). RankL deficient mice have very few M cells but
71 exogenous administration of recombinant RankL was able to mitigate that loss (Knoop et al., 2009).
72 RankL binding to Rank receptor leads to the activation of the intracellular adaptor molecule of
73 RANK; TRAF6 which in turn leads to activation of both canonical (RelA/p50 heterodimer) and non-
74 canonical NF- κ B (RelB/p52 heterodimer) activation (Lernbecher et al., 1994; Walsh et al., 2014,
75 Kanaya et al., 2018). The canonical RelA/p50 activation led to expression of early M cell markers
76 like MarcksL1 and CCL9 whereas non-canonical RelB/p52 activation led to expression of Spi-B and
77 Sox8 transcription factors, both deemed essential to maturation of M cells (Kanaya et al., 2018;
78 Kimura et al., 2019). Along with RankL, expression of Spi-B and Sox8 are essential for the
79 development of Gp2 positive M cells. Both Spi-B and Sox8 mutant mice exhibited the absence of
80 mature M cells with Gp2 whereas MarcksL1⁺AnnexinV⁺ immature M cells were intact (de Lau et al.,
81 2012; Kanaya et al., 2012; Kimura et al., 2019; Sato et al., 2013). Spi-B ^{-/-} still showed Sox8
82 expression and Sox8 ^{-/-} mice expressed Spi-B and even though both mice had activation of both NF-
83 κ B transcription pathway, p50/RelA and p52/RelB, they still showed an immature M cell phenotype
84 lacking the expression of Gp2 (Kanaya et al., 2018). Taken together, despite their critical role in the
85 onset of mucosal immune responses, M cell development and their differentiation into maturity have
86 not yet been fully characterized partly due to their rarity in the gastrointestinal tract (Kanaya & Ohno.,
87 2014). Importantly, the sole overexpression of Spi-B and Sox8 are not sufficient for the induction of
88 GP2 receptor i.e., M cell maturation, suggesting that additional M cell specific transcription factors
89 are needed (Kimura et al., 2019).

90 Intestinal cell differentiation, development and functionality are regulated by several factors, one of
91 the indispensable ones being Polycomb Group (PcG) proteins. PcG proteins are essential for
92 embryonic stem cell self-renewal and pluripotency but they are also necessary for the maintenance
93 of cell identity and cell differentiation throughout life (Schuettengruber & Cavalli, 2009). They

94 broadly form three groups of polycomb repressive complexes (PRCs) known as PRC1, PRC2 and
95 Polycomb Repressive DeUBiquitinase, each of these complexes reassemble chromatin by explicitly
96 defined mechanisms that involve variable configurations of core and accessory subunits. This
97 configuration is demonstrated by the way PRC2 catalyzes trimethylation of histone H3 lysine 27
98 (H3K27me3) and presents a binding site for PRC1 in embryonic stem cells (Cao et al., 2002). Lee et
99 al showed that PRC2 played a repressive role of expression of developmental regulators necessary
100 for cell differentiation (Lee et al., 2006). Interestingly, genes critical for cell identity lose their
101 methylation on H3 lysine K27 whereas genes that regulate alternate cell types keep their methylation
102 and remain repressed (Bernstein et al., 2006). In human embryonic stem (ES) cells, Wnt-signaling
103 genes are bound by PRC2, analogously this is also exhibited in adult tissues for instance in
104 adipogenesis (Wang et al., 2010). The integrity and homeostasis of healthy intestine is partly
105 regulated by canonical Wnt signaling and it has also been shown that secretory and absorptive
106 progenitor cells show comparable levels of histone modifications at most of the same cis elements in
107 the genome (T. H. Kim et al., 2014). Our study and others (Chiacchiera et al., 2016; Oittinen et al.,
108 2017; Vizán et al., 2016) found out how PRC2 regulates a substantial subset of genes that were
109 involved in canonical Wnt signaling and contributed to the differentiation of Lgr5 expressing stem
110 cells to secretory and absorptive cell types in the intestine.

111 To further understand the complexity of M cell differentiation, we asked if PRC2 regulates M cell
112 differentiation. We used high-throughput tools such as Chip- seq and Gro-seq to identify factors that
113 contribute to the function and development of M cells in the intestine. We identified a total of 12 TFs
114 that are regulated by PRC2 exclusively during M cell differentiation of which 6 were downregulated
115 and 6 were upregulated. One of the M cell specific TF, *Esrrg*, was found to be essential for the
116 differentiation of mature Gp2+ M cells in vitro. We found that *Esrrg* was expressed exclusively in M
117 cells in Peyer's patches and was shown critical for the activation of Sox8 transcription factor. *Esrrg*
118 expression was intact even in Sox8 deficient mice and was dependent on the activation of non-

119 canonical NF- κ B signaling. These observations illustrate that *Esrrg* is a crucial player in the
120 differentiation and functionality of a mature Gp2⁺ M cell.

121

122 **Results**

123 **PRC2 is not restricting M cell differentiation**

124 We and others have previously shown that disrupting PRC2 activity leads to a precocious expression
125 of terminal differentiation markers of intestinal enterocytes (Benoit et al., 2013; Oittinen et al., 2017;
126 Vizán et al., 2016). Moreover, PRC2 has been shown to preserve intestinal progenitors and restricting
127 also secretory cell differentiation (Chiacchiera et al., 2016). Contrary to absorptive cell differentiation
128 (ENRI), when organoids were treated with RANKL the level of expression of PRC2 members *Ezh2*
129 and *Suz12* were comparable to the levels in organoids grown in standard organoid culture media
130 (ENR500) (Fig. 1A). Next, we asked if PRC2 inhibition (Fig. 1B) can augment M cell differentiation
131 and we saw that, contrary to enterocyte differentiation, expression of all M cell markers are
132 downregulated when the activity of PRC2 is pharmacologically inhibited during the RANKL-induced
133 M cell differentiation (Fig. 1C).

134

135 **PRC2 regulated genes during M cell differentiation**

136 It has been previously shown that PRC2 regulates transcription factors necessary to intestinal stem
137 cell maintenance and differentiation e.g., *Ascl2* (Schuijers et al. 2015 & Oittinen et al. 2017) and
138 *Atoh1* (Chiacchiera et al. 2016). Since PRC2 mainly regulates genes involved in development or
139 signaling (Ram et al. 2011 Cell) we reasoned that identifying genes regulated by PRC2 during M cell
140 differentiation might reveal gene network necessary to this cell type in the intestine. M cell
141 differentiation was induced in mouse intestinal organoids with RankL and gene expression was

142 analysed with Gro-Seq and PRC2 target genes identified with ChIP-seq by using H3K27me3
143 antibody. Genes differentially expressed after RankL treatment are shown in figure 2A. ChIP-seq
144 performed with H3K27me3 antibody revealed a significant number of genes regulated by PRC2 for
145 M cell differentiation. When comparing our 3 different Chip-seq's (WENRC – stem cell conditions;
146 ENRI – enterocyte condition; RankL – M cell differentiation), we observed that in M cells, 38 (9.2%)
147 and 35 (10.3%) of genes were upregulated but silenced by PRC2 in WENRC and ENRI, respectively.
148 32 PRC2-target genes were uniquely upregulated during M cell differentiation and not in enterocyte
149 differentiation. 46 (27.7%) and 52 (11.5%) PRC2-target genes were silenced in organoids treated
150 with RANKL but expressed in WENRC and ENRI, respectively. 42 genes were uniquely silenced in
151 M cell but not in enterocyte differentiation. PRC2 target genes are shown in figure 2 B-D and the M
152 cell specific accumulation and ablation of H3K27me3 signal in the gene promoters are shown in
153 figure 2E. Gene ontology analyses indicate that PRC2 regulate many DNA-binding transcription
154 factors during the M cell differentiation (Fig. 2F). Total of 12 transcription factors were differentially
155 expressed: six were silenced by PRC2 in M cells and six were specifically expressed in M cells but
156 repressed by PRC2 in organoids grown both in stemness and enterocyte conditions. The six PRC2-
157 target genes specifically expressed in M cells are Sox8, Atoh8, Esrrg, Smad6, Maf and Zfp819. The
158 six genes silenced are Hoxb5, Hoxb9, Sp9, Sp5, Nr4a1 and Atf3.

159 160 **Esrrg is expressed in M cells and induced by Rank-RankL signalling**

161 Of the six transcription factors that were specifically expressed in M cells in PRC2-dependent manner
162 (Fig. 2 A&B), Estrogen related receptor gamma (Esrrg) turned up as one of the most highly expressed
163 PRC2-regulated gene during M cell differentiation. (log2 fold changes –6.64 RankL vs. ENRI and –
164 4.76 in RankL vs. WENRC comparisons) (Fig. 3A). Immunohistochemistry analysis for Esrrg in
165 Peyer's patch shows that Esrrg was localized in the FAE cells (Fig. 3B). RNA was isolated from FAE
166 isolated from Peyer's patch and villus epithelium and the RT-qPCR analysis confirmed that the Esrrg

167 was significantly enriched in FAE (GP2 as a marker) when compared to villus epithelium (Fig 3C).
168 To ascertain that *Esrrg* is a novel RankL-induced M cell gene, RT-qPCR analyses was performed for
169 organoids before and after 4 days of RankL treatment. The expression of *Esrrg*, together with M cell
170 marker *Gp2*, was significantly induced with RankL treatment (Fig. 3D). To confirm that *Esrrg*
171 expression was specifically regulated by Rank-Rankl signalling, we generated Rank-deficient mouse
172 intestinal organoids using Lenti-V2 CRISPR/Cas9 system and found that in Rank-deficient
173 organoids, RankL treatment did not induce the expression of *Esrrg* (Fig. 3E). The Rank KO was
174 validated by immunoblot analysis (supplemental Fig 2A)

175

176 **Non-canonical NF- κ B activation is necessary and sufficient for *Esrrg* expression**

177 Rank-RankL signaling has been previously shown to activate canonical as well as non-canonical NF-
178 κ B pathways. LT β R signaling was implicated in inducing both classical p50–RelA and non-canonical
179 p52–RelB heterodimers in Peyer’s patch (Yilmaz et al.,2003). Mouse intestinal organoids were grown
180 for 3 days in the presence of LT α 1 β 2, the ligand of LT β R, and we observed that, similar to *Spi-B*,
181 *Esrrg* expression was also significantly increased (Fig 4A). To identify if canonical NF- κ B
182 specifically had a role in *Esrrg* expression, mouse organoids were grown in the presence and absence
183 of RankL and SC-514, a specific inhibitor of I κ B kinase- β (Kishore et al., 2003). We found that
184 inhibiting canonical NF- κ B with SC-514 completely abrogated the expression of *Esrrg* (Fig 4B),
185 similarly as was reported for the *Spi-B* (Kanaya et al., 2018). Both, p50-RelA and p52-RelB
186 overexpression led to increased expression of *Esrrg* (Fig 4C). It was previously demonstrated that
187 p50/RelA (canonical NF- κ B) directly targets the transcription of RelB (Bren et al., 2001). The
188 treatment of p52/RelB overexpression organoids with SC-514 could not suppress the activation of
189 *Esrrg* (Fig. 4D). To conclude, these data indicate that non-canonical NF- κ B is necessary and sufficient
190 to induce *Esrrg*.

191

192 **Esrrg expression is required for Sox8 activation and maturation of M Cells**

193 Given that *Esrrg* was prominently expressed in Peyer's patches and regulated by non-canonical Nf-
194 kb expression, we sought to see if abolition of *Esrrg* had any effect on M cell differentiation and
195 development. To investigate this, mouse intestinal organoids deficient in *Esrrg* were generated by
196 LentiCRISPR V2 CRISPR-Cas9 genome editing. Targeting of *Esrrg* by the gRNA selected (Fig. 5A)
197 resulted in a significant reduction in expression of *Esrrg* protein (Fig 5B). *Esrrg* deficient organoids
198 were grown in the presence and absence of RankL for 3 days. RT-qPCR analysis revealed that *Gp2*
199 was nearly absent and *Sox8* expression was significantly reduced in *Esrrg* targeted organoids (Fig.
200 5C). *Gp2* and *Sox8* immunostaining in *Esrrg* targeted organoids showed an absent and reduced
201 expression respectively (Fig 5D). However, expression of *Spi-B* and *Tnfaip2* remained unaffected in
202 the *Esrrg* deficient organoids (Fig 5C and 5E). Early M cell differentiation markers such as *CCL20*,
203 *CCL9* and *MarksL1* were significantly affected by the lack of *Esrrg* as well (Fig 5E). *Aif1*, which is
204 a regulatory gene for transcytosis in M cells was also found to be severely affected by lack of *Esrrg*
205 expression (Fig 5E). Our observations show that *Esrrg* is required for the expression of *Sox8* and for
206 the early markers as well as late maturation steps in M cell differentiation. To validate for off-target,
207 we knocked out *Esrrg* with a second guide RNA, comparable results were observed (Supplementary
208 Figure 1A and 1B).

209

210 **Esrrg acts upstream of Sox8 expression**

211 *Spi-B* and *Sox8* were found to be two key transcription factors involved and essential for M cell
212 differentiation and regulation of expression of other M cell associated genes (de Lau et al., 2012;
213 Kanaya et al., 2012; Kimura et al., 2019; Sato et al., 2013). *Spi-B* and *Sox8* mutant mice lacked *Gp2*+
214 mature M cells and were unable to transcytose antigens. However, it was observed that *Spi-B* was

215 dispensable to the expression of Sox8 even though Spi-B expression was moderately reduced in the
216 Sox8 mutant mice (Kimura et al., 2019). To investigate if Esrrg is affected by knockout of Sox8,
217 RNA was isolated from FAE of Peyer's patch from Sox8 +/+ and Sox8 -/- mice. RT-qPCR analysis
218 of FAE's from PP's of Sox8 +/+ and Sox8 -/- demonstrated that the expression of Esrrg remained the
219 same and even higher in Sox8 -/- mice (Fig. 6A). Organoids isolated from Sox8 +/+ and Sox8 -/-
220 mice were treated with RankL and expression of Esrrg expression was analysed by RT-qPCR and
221 Western blot. The analysis showed Esrrg expression was intact and similar to the in vivo data (Fig.
222 6B and 6C). This suggests that Esrrg acts upstream of Sox8 and could play a role in the activation of
223 Sox8. Next, we explored how Esrrg was affected by Spi-B. Spi-B deficient organoids were generated
224 by LentiCRISPR V2 genome editing and grown in the presence and absence of RankL. qPCR analysis
225 showed that Esrrg was moderately affected by the lack of Spi-B (Fig 6D). Western blot analysis also
226 indicated that Esrrg was expressed less in Spi-B deficient organoids (Fig 6E) Spi-B Ko organoids
227 were validated by immunoblot analysis (supplemental Fig 2B).

228

229 **Overexpression of Esrrg is not sufficient for GP2+ M cells but Esrrg agonist augmented GP2** 230 **expression**

231 Spi-B expression in Sox8 KO mice and Sox8 expression in Spi-B KO mice did not lead to a mature
232 GP2 M cell phenotype in either of these mice . As we found that the expression of Gp2 was dependent
233 on Esrrg (Fig. 5C) we sought to investigate if the overexpression of Esrrg alone could lead to
234 upregulation of Sox8 or Gp2 expression. Esrrg cloned into CSII-CMV-MCS-IRES2-Bsd
235 overexpression vector was transduced into mouse intestinal organoids. RT-qPCR analysis showed
236 that Esrrg alone was not adequate enough to induce Gp2 or other M cell specific transcription factor
237 such as Spi-B or Sox8. (Fig 7A). Esrrg is an orphan nuclear receptor without known natural ligands.
238 However, 4-hydroxytamoxifen (4OHT) has been shown to bind and inhibit Esrrg activity and
239 phenolic acyl hydrazones- GSk4716 has been identified as an agonist that enables the activation of

240 other co-activators and other downstream targets (Coward et al., 2001.; Zuercher et al., 2005). The
241 antagonist 4OHT along with RankL induced a similar result to the lack of Esrrg protein, Spi-B
242 remained unaffected, whereas Sox8 and Gp2 were significantly affected (Fig 7B). Organoids treated
243 with agonist GSK4716 and RankL did not show significant increase in Sox8 or Spi-B expression
244 however, Gp2 expression was slightly augmented with GSK4716 (Fig 7C).

245

246 **Discussion**

247 Our data reveals the PRC2-regulated genes during the differentiation of intestinal microfold cells. As
248 PRC2 is the master regulator of development it is very likely that many of the identified PRC2 targets,
249 that are specifically induced in M cells, contributes to the maturation of this cell type. Transcription
250 factors are usually expedient to development and we identified six PRC2 regulated transcription
251 factors specifically upregulated after the RankL-induced M cell differentiation. Amongst those was
252 previously identified transcription factor Sox8 (Kimura et al, 2019) which we also here showed to be
253 necessary to M cell differentiation. As Esrrg was clearly the most highly induced PRC2-target gene
254 during the M cell differentiation, we pursued to study it in more detail in intestinal organoids and
255 showed that it is indispensable to the maturation of intestinal stem cells into Gp2+ M cells. Esrrg is a
256 member of the ESRR nuclear receptor family which also includes ESRR A and ESRR B (Giguère,
257 2002). This subfamily of orphan nuclear receptors has shown to share target genes, coregulatory
258 ligands, and sites of action with ERs. Esrrg was implicated to control macrophage function indirectly
259 through regulation of intracellular iron. In response to *Salmonella typhimurium* infection, hepatic
260 expression of the hormone hepcidin is upregulated by ER γ downstream on IL-6 signalling (Bren et
261 al., 2001; D. K. Kim et al., 2014). However, no prior data about the expression and function of Esrrg
262 in M cell and M cell induced transcytosis of antigens exist. We defined the specific expression of
263 Esrrg by M cells in mouse FAE's and how its expression was upregulated by induction of RankL and

264 was under the influence of RankL-Rank pathway. The loss of *Esrrg* led to lack of expression of GP2
265 receptor in *Esrrg* KO organoids which is characteristic of a mature M cell and lack of Gp2 in M cell
266 has been shown to result in attenuation of antigen sampling and transcytosis. This distribution of
267 *Esrrg* along with the phenotype of *Esrrg* KO organoid highlights a critical role for *Esrrg* in the
268 maturation of functional M cells

269 RelB/p52 was shown to upregulate Spi-B (Kanaya et al., 2018). Similarly, here we show that *Esrrg*
270 is also regulated by the activation of the non-canonical NF- κ B pathway. We believe that the
271 expression of *Esrrg* and Spi-B is regulated downstream parallelly by RankL-Rank-RelB/p52
272 signalling (Fig. 8). *Esrrg* has been shown to behave as a constitutive activator of transcription.
273 (Matsushima et al., 2007). Here we demonstrate that *Esrrg* is needed for the activation of Sox8.
274 Kimura et al previously showed how Sox8 was indispensable for the expression of Gp2 and Sox8 KO
275 mice showed a decrease in uptake of antigens and a significant decrease of IgA+ immunoglobulins.
276 Sox8 was also shown to bind directly to Gp2 promoter along with SpiB. The significant decrease in
277 Sox8 expression could explain as to why *Esrrg* KO organoids were not able to activate Gp2. Sox8
278 expression alone cannot lead to an increase in Gp2 expression because enhancer activation by SOX
279 proteins require DNA binding partners specific for each member of the SOX family. These DNA
280 binding partners aid in stabilizing the SOX family to their target regions (Kamachi et al., 1999). This
281 suggests that *Esrrg* activated Sox8 requires another molecule downstream of Spi-B or through another
282 pathway to bind to Gp2 to induce its expression, however further exploration is required to confirm
283 this. *Esrrg* overexpression alone did not lead to expression of Sox8 confirming the need of a ligand
284 and/or other factors to activate downstream targets.

285 A major portion of our investigation of *Esrrg* in M cells was conducted in vitro and *Esrrg* ablation in
286 mouse models is required to further ascertain its role. Interestingly, Sox8 deficiency did not affect
287 early M cell markers, however, *Esrrg* KO organoids showed a drastic decrease in expression of early
288 M cells markers such as CCL9 and MarcksL1. Mature marker Gp2 receptor expression was

289 significantly decreased as well. The loss of Aif1 expression in Esrrg knockout means that transcytotic
290 capacity of the M cells would be affected as well. In the Sox8 KO mice, we observed that Esrrg
291 expression was still intact and even observed to have a higher expression in vivo and in vitro
292 suggesting that Esrrg was not affected by the absence of Sox8 and acts upstream of it. The significance
293 of Esrrg was further confirmed with our antagonist and agonist experimental study. Even though
294 tamoxifen is known to trigger multiple signalling pathways in the cell, it has been identified as an
295 antagonist for Esrrg receptor, tamoxifen 1um was enough to significantly decreased the expression
296 of Gp2 and Sox8 similar to the Esrrg KO organoids. The treatment of intestinal organoids with RankL
297 and Esrrg agonist GSK4716 augmented the expression of Gp2 when compared to organoids with just
298 RankL treatment. This could be because GSK4716 binds to Esrrg and activates several other unknown
299 downstream targets that combine to attenuate Gp2 expression. Esrr family members are known to be
300 orphan receptors meaning they might not need a ligand for its function, or the ligand remains
301 unknown. Overexpression of Esrrg did not lead to an increase in Sox8 expression or other
302 transcription factors necessary for mature M cell differentiation presumably because a specific ligand
303 might be necessary. However further studies are needed to prove this.

304 In conclusion, we identified several previously unknown PRC2 regulated genes implicated in M cell
305 differentiation. One of the genes, we identified, Esrrg, is as a key transcription factor required for the
306 functional development and M cell differentiation which is pertinent for constant surveillance of the
307 mucosal lining of the gastrointestinal tract. We believe that the further exploration of other activators
308 of Gp2 will lead to better elucidation of M cell maturation and antigen transcytosis. This will create
309 potential to provide strategic innovation in support of mucosal/oral vaccine advancement.

310

311

312

313 **Materials and Methods**

314

315 **Animals.** C57BL/6JRj mice were purchased from Janvier labs and were maintained with constant
316 breeding. The *Bac-Cre-ERT2;Sox9^{ff};Sox8^{-/-};Rosa26^{Eyfp}* mice were a gift from Raphael Jimenez
317 (Granada, Spain). These mice were backcrossed with C57BL/6JRj to isolate Sox8^{-/-} allele. Sox8^{+/-}
318 were bred to obtain Sox8^{-/-} and littermate controls: Sox8^{+/-} and Sox8^{+/+}. F1-4 mice were used for
319 gene or protein expressions. Genotyping of the wild-type, heterozygous, and deleted alleles was
320 carried out by PCR with the following primers: F1, 5'-GTCCTGCGTGGCAACCTTGG-3'; R1, 5'-
321 GCCCACACCATGAAGGCATTC-3'; F3, 5'-TAAAAATGCGCTCAGGTCAA-3'. Conventional
322 conditions were observed for the maintenance of these mice at the pathogen free animal facility of
323 the faculty of Medicine and Health Technology. All animal experiments were approved by the Finnish
324 National Animal Experiment Board (Permit: ESAVI/5824/2018).

325

326 **Intestinal Organoid culture.** Intestinal crypt isolation and culture techniques were observed as
327 previously described by Sato et al 2011 and de Lau et al 2012. Mouse duodenum were cut
328 longitudinally, and the villi were gently scraped off with 2 glass slides. After a couple of PBS washes,
329 they were cut into 2mm pieces and pipetted up and down 5 times in 15ml PBS with a 10ml pipette,
330 this step was repeated 3 times with fresh PBS. The pieces were incubated in 10mM EDTA in PBS
331 for 20 minutes rocking at room temperature. The pieces were vigorously suspended in cold PBS and
332 the mixture was strained through a 70- μ m cell strainer (Fisher Scientific). This mixture was enriched
333 to crypt fraction through centrifugation at 150 x g for 5 minutes. The enriched crypts were embedded
334 in Matrigel (Corning) and 30ul were plated on a 24 well plate. Crypts were cultured in an optimal
335 medium consisting of advanced DMEM/F12 (Thermo Fisher Scientific) that contained HEPES
336 (10mM, Sigma-Aldrich), Glutamax (2mM, Thermo Fisher Scientific), Penicillin-streptomycin
337 (100U/ml, Sigma-Aldrich), B-27 supplement minus Vitamin A (Thermo Fisher Scientific), N-2

338 supplement (Thermo Fisher Scientific), *N*-acetylcysteine (1 mM; Sigma-Aldrich), recombinant
339 murine EGF (50 ng/mL; Thermo Fisher Scientific), recombinant murine Noggin (100 ng/mL;
340 PeproTech), recombinant mouse R-spondin1 (1 µg/mL; R&D Systems). Media were changed every
341 2 days. For M cell differentiation, recombinant mouse RankL (100ng/ml, Peprotech) was added to
342 the media and incubated for 4 days. PRC2 was inhibited by addition of 5µm of Ezh2 inhibitor (EI1)
343 (CAS 1418308-27-6 Calbiochem Chemicals). For activation of NF-κB, human LTα1β2 (1 µg/ml,
344 R&D) were added into organoid cultures. Restriction of IκB kinase-β activity was achieved by
345 adding, SC-514 (125 µM Calbiochem) for 3 days (Akiyama et al., 2008). (Z)-4-Hydroxytamoxifen
346 (1µm, Sigma-Adrich) was used as an antagonist of Esrrg and GSK 4716 (10 µm, Sigma-Aldrich) was
347 used as an agonist of Esrrg.

348 **ChIP-Seq analysis.** Intestinal organoids (in ENR500, ENRI and RankL culturing conditions) were
349 isolated from Matrigel with Cell Recovery Solution (Corning). This was followed by washes with
350 cold PBS and dissociation into single cell suspension using TrypLE Express (Thermo Fisher
351 Scientific) and counted. 10×10^6 of cells of each condition were crosslinked with formaldehyde,
352 after which nuclei were isolated with Lysis buffer 1, 2 and 3 as described (Lee et al., 2006) and
353 sonicated with a Covaris S220 ultrasonicator (Woburn, MA). The resulting nuclear extract was
354 incubated with Dynal protein G beads which were preincubated with 5µg of H3K27me3 or H3
355 antibody (ab6002 and ab1791, Abcam) respectively at 4°C overnight. After washing and elution of
356 bound complexes from the beads, crosslinks were reversed by heating to 65°C. IP and input DNA
357 were then purified by a treatment with RNase A, proteinase K, and phenol:chloroform extraction.
358 NEBnext UltraDNA-library preparation kit for Illumina (NEB, Ipswich, MA) was used to construct
359 libraries from IP and input DNA and subjected to 50 bp single-end read sequencing with Illumina
360 Hiseq 2000 at EMBL Genecore, Heidelberg, Germany.

361 **Gro-Seq analysis.** ENR500 and RankL treated organoids were harvested (as in ChIP-Seq) and GRO-
362 Seq was performed for equal number of isolated nuclei. Nuclei extraction and run on reaction was

363 performed as described (Core LJ et al., 2008). For each replicate, 3 million cells were suspended to a
364 final volume of 80-200 μ l of freezing buffer. Trizol LS (Life Technologies) was used to extract RNA
365 and fragmented for 13 mins in 70°C using RNA Fragmentation Reagents (Life Technologies) and
366 later purified by running through RNase-free P-30 column (Bio-Rad, Hercules, CA). PNK was used
367 to dephosphorylate RNA for 2 hours (New England Biolabs, Ipswich, MA) followed by heat-
368 inactivation. 65 μ l of blocking solution was added (5x volume of 0.25xSSPE, 1 mM EDTA, 37.5 mM
369 NaCl, 0.05% Tween-20, 0.1%PVP and 0.1% ultrapure BSA for 1 hour in RT), the anti-BrdU bead
370 slurry (Santa Cruz Biotech) suspended in 500 μ l of binding buffer (0.25xSSPE, 1 mM EDTA, 37.5
371 mM NaCl 0.05% Tween-20) was used to purify the dephosphorylated reaction. After binding for an
372 hour in RT, the beads were washed 2x with binding buffer, 2x with low salt buffer (0.2xSSPE, 1mM
373 EDTA, 0.05% Tween-20), 1x with high salt buffer (0.2xSSPE, 1mM EDTA, 135 mM NaCl 0.05%
374 Tween-20) and lastly 2x with TE-buffer (1xTE, 0.05% Tween-20). The elution of the RNA was
375 completed with 130 μ l of elution buffer (50 mM Tris-HCl pH 7.5, 150 mM NaCl, 0.1% SDS, 1mM
376 EDTA, and 20 mM DTT) followed by ethanol precipitation overnight. All buffers were supplemented
377 with SUPERase In (2 μ l /10 ml; Life Technologies). Library preparations were performed the next
378 day as previously reported by Kaikkonen Mu et al 2014. The library was amplified with 14 cycles
379 and the final product of 190-135 bp was extracted from a 10% TBE gel. The DNA was purified from
380 the gel using the Gel extraction Kit (Thermo) and eluted in TE buffer (TE 0.1% Tween + 150 mM
381 NaCl). ChIP DNA clean & Concentrator Kit (Zymo Research Corporation, Irvine, CA) was used to
382 purify the library, the DNA was quantified with the Qubit fluorometer and sequenced with Illumina
383 HiSeq 2000 at EMBL Genecore, Heidelberg, Germany.

384 **ChIP- and Gro-Seq data analyses.** Analyses were performed as described by Core LJ et al 2008,
385 Kaikkonen Mu et al 2014, and Oittinen et al 2016. The data has been deposited in the NCBI Gene
386 Expression Omnibus database (GSE157629). Gro- and ChIP-seq data for the individual genes are
387 shown in Supplementary tables 1 and 2 respectively.

388 **Immunohistochemistry and immunofluorescence.** Peyer's patches from the ileum were isolated
389 and washed with cold PBS and embedded into paraffin blocks. Sections from the blocks were
390 rehydrated and washed with PBS. After incubation with 1% PBS/BSA supplemented with 5% normal
391 donkey serum for blocking. Antigen retrieval was processed with citrate buffer, pH 6.0 (121°C for 5
392 min) and stained overnight at 4°C for Esrrg (abcam, ab49129), Gp2 (MBL, D278-3) antibodies. This
393 was followed by anti-Rabbit secondary for Esrrg and Anti-Rat secondary for Gp2. The sections were
394 examined with a light microscope. For whole-mount immunostaining, crypt organoids were plated in
395 an 8-well chamber and cultured for 4 days after which they were fixed with 4% PFA, followed by
396 permeabilization with 0.1% Triton X-100. The organoids were stained with the following primary
397 antibodies overnight at 4°C: rabbit anti-Spi-B (Spi-B (D3C5E), CST, 14223), rabbit anti-Sox8
398 (abcam, ab221053), rat anti-Gp2 (MBL, D278-3). This was followed by incubation with secondary
399 antibody anti-rabbit Alexa fluor 568 for Spi-B and Sox8 and anti-Rat Alexa fluor 488 for Gp2. Cells
400 were analyzed with Nikon A1R+ Laser Scanning Confocal Microscope after mounting with ProLong
401 Diamond with Dapi mounting solution (Molecular Probes P36962).

402 **Isolation of villous epithelium and follicle associated epithelial cells.** Villous Epithelium (VE) and
403 Follicle Associated Epithelium (FAE) were prepared by isolating illeal PP's and small pieces of ileum
404 from the intestine. These pieces were washed in cold PBS and later incubated in 30mM EDTA, 5mM
405 DTT in PBS and gently shaken in ice on a rocker for 20 minutes. After which surrounding epithelial
406 cells were peeled off from lamina propria and PP's. FAE was carefully cleaned off from surrounding
407 VE tissues with a 26-gauge needle under a stereo microscope.
408

409 **CRISPR–Cas9 gene editing of intestinal organoids.** Guide RNA's for Rank, Spi-B and Esrrg were
410 designed with CRISPR design tool (<http://crispr.mit.edu>). (Shalem, O. et al. *Science* 343, 84–87
411 (2014)). The guides were cloned into lentiCRISPR v2 vector (Addgene, 52961). The cloned vector
412 was transfected into 293FT cells (ThermoFisher R7007) and the supernatant was collected at 48 hours
413 and concentrated with Lenti-X concentrator (Clontech). The 293FT cell line was found to be negative
414 for mycoplasma. Cultured intestinal organoids were grown in ENCY (EGF, Noggin, Chir-99021 and
415 Y-27632) 2 days prior to transduction. Organoids were dissociated into single cells mechanically
416 along with TrypLE Express (Thermo Fisher Scientific) supplemented with 1,000 U/ml DnaseI for 5
417 min at 32 °C. The single cell suspension was washed once with Advanced DMEM and resuspended
418 in transduction medium (ENR media supplemented with 1mM nicotinamide, Y-27632, Chir99021, 8
419 µg/ml polybrene (Sigma-Aldrich) and mixed with concentrated virus. The cell-virus mixture was
420 spinoculated 1 h at 600 x g 32 °C followed by 2–4 h incubation at 37°C, after which they were
421 collected and plated on 60% Matrigel overlaid with transduction medium without polybrene.
422 Transduced organoids were selected with 2 rounds of 2 µg/ml of puromycin (Sigma-Aldrich) on day
423 2 and day 4, after which clones were expanded in maintenance ENR medium. Knockout was
424 confirmed by western blot to check for the expression of deleted gene.

425 Oligonucleotides used for generation of gRNAs: Esrrg (1)

426 CACCGTCTGTCAAGACGGACCCCTG, AACCAGGGGTCCGTCTTGACAGAC, Esrrg (2)

427 CACCGTGGCGTCCGAAGACCCACCA; AAACCAGGGGTCCGTCTTGACAGAC. Spi-B (1)

428 CACCGAGACTCCTTCTGGGTACTGG, AAACCCAGTACCCAGAAGGAGTCTC; Rank (1)

429 CACCGAAAGCTAGAAGCACACCAG, AACCTGGTGTGCTTCTAGCTTTC.

430 **Lentivirus infection for overexpression.** RelB, p52, RelA, p50 plasmids were a gift from Hiroshi
431 Ohno's lab (RCIMS, Kangawa, Japan) and Esrrg cDNA was cloned by Twist bioscience (California,
432 USA). These were cloned into CSII-CMV-MCS-IRES2-Bsd vector which was kindly provided by
433 the RIKEN bioresource center Japan and Hiroyuki Miyoshi. The same protocol for Crispr-Cas9

434 lentiviral generation and transduction was followed and cells were embedded into Matrigel and
435 incubated for 2-3 days.

436 **Immunoblotting.** Organoids were recovered from Matrigel with Cell Recovery media (Corning).
437 Organoids were washed with PBS and the cells were lysed with 2x Laemmli solution and boiled at
438 98 degrees. Protein concentrations were measured by Pierce 660nm Protein Assay Reagent and IDCR
439 (ThermoFisher Scientific,22660). Samples were loaded equally in terms of protein concentration into
440 10% Bis-Tris protein gels (Life Technologies) and blotted on nitrocellulose membranes. Membranes
441 were incubated with primary antibodies: Anti-Esrrg (abcam, ab49129); Anti-Spi-B (Spi-B D4V9S,
442 CST 14337); Anti-H3K27me3 (abcam, ab192985); Anti-H3 (abcam, ab1791), Anti-Rank
443 (MyBioSource, MBS9133424), Anti-GAPDH (abcam, ab8245) at 4 °C overnight, and HRP-
444 conjugated anti-rabbit (Sigma-Aldrich; 1:5000) or anti-mouse (CST; 1:1000) for 1 h at room
445 temperature. Signal was detected using ECL reagent (Amersham 2232).

446 **Real-time quantitative reverse transcription PCR.** Total RNA was prepared using TRIzol (Life
447 Technologies) from intestinal organoids and epithelium isolated from mice. Isolated RNA was
448 transcribed to first strand cDNA using iScript cDNA synthesis Kit (Biorad, 1708891). qPCR
449 amplification was detected using Ssofast evergreen supermixes (Biorad,172-5203). The specific
450 primers used, are listed in the supplementary data.

451

452 **Data availability.** The GhIP- and Gro-seq data have been deposited in the NCBI Gene Expression
453 Omnibus database (GSE157629).

454

455 **Acknowledgements**

456 We would like to thank Rafael Jiménez for providing Sox8^{-/-} mouse transgenic line. This work was
457 supported by the Academy of Finland (no. [310011](#)), Tekes (Business Finland) (no. [658/31/2015](#)),
458 Paediatric Research Foundation, Sigríd Jusélius Foundation, Mary och Georg C. Ehrnrooths Stiftelse,
459 Laboratoriolääketieteen Edistämmissäätiö sr. The funding sources played no role in the design or
460 execution of this study or in the analysis and interpretation of the data.

461 **Author contributions**

462 JJG, KV: Study concept and design. JJG, LMD, VZ, SI, TR, FTAM, HN: experiments and acquisition
463 of data. MO: bioinformatic analyses. JJG, LMD, KV: analysis and interpretation of data. JJG, MO,
464 KV: manuscript drafting. SI, PK, HN, MK: data curation & reviewing the manuscript KV: project
465 administration and funding acquisition. JJG, MO, LMD, VZ, SI, TR, FTAM, HN, PK, MK, KV:
466 critical revision of the manuscript for important intellectual content. All authors approved the final
467 version of the manuscript.

468 **Conflict of interest**

469 None

470

471 **References**

- 472 Benoit, Y. D., Laursen, K. B., Witherspoon, M. S., Lipkin, S. M., & Gudas, L. J. (2013). Inhibition
473 of PRC2 histone methyltransferase activity increases TRAIL-mediated apoptosis sensitivity in
474 human colon cancer cells. *Journal of Cellular Physiology*, 228(4), 764–772.
475 <https://doi.org/10.1002/jcp.24224>
- 476 Bernstein, E., Duncan, E. M., Masui, O., Gil, J., Heard, E., & Allis, C. D. (2006). Mouse Polycomb
477 Proteins Bind Differentially to Methylated Histone H3 and RNA and Are Enriched in Facultative
478 Heterochromatin. *Molecular and Cellular Biology*, 26(7), 2560–2569.
479 <https://doi.org/10.1128/mcb.26.7.2560-2569.2006>
- 480 Bren, G. D., Solan, N. J., Miyoshi, H., Pennington, K. N., Pobst, L. J., & Paya, C. V. (2001).
481 Transcription of the RelB gene is regulated by NF-κB. *Oncogene*, 20(53), 7722–7733.
482 <https://doi.org/10.1038/sj.onc.1204868>

- 483 Cao, R., Wang, L., Wang, H., Xia, L., Erdjument-Bromage, H., Tempst, P., Jones, R. S., & Zhang,
484 Y. (2002). Role of histone H3 lysine 27 methylation in polycomb-group silencing. *Science*,
485 298(5595), 1039–1043. <https://doi.org/10.1126/science.1076997>
- 486 Chiacchiera, F., Rossi, A., Jammula, S., Zanotti, M., & Pasini, D. (2016). PRC 2 preserves intestinal
487 progenitors and restricts secretory lineage commitment . *The EMBO Journal*, 35(21), 2301–
488 2314. <https://doi.org/10.15252/embj.201694550>
- 489 Core, L. J., Waterfall, J. J., & Lis, J. T. (2008). Nascent RNA sequencing reveals widespread pausing
490 and divergent initiation at human promoters. *Science*, 322(5909), 1845–1848.
491 <https://doi.org/10.1126/science.1162228>
- 492 Coward, P., Lee, D., Hull, M. V, Rgen, J., & Lehmann, M. (n.d.). *4-Hydroxytamoxifen binds to and*
493 *deactivates the estrogen-related receptor*. Retrieved September 29, 2020, from
494 www.pnas.org/cgi/doi/10.1073/pnas.151244398
- 495 de Lau, W., Kujala, P., Schneeberger, K., Middendorp, S., Li, V. S. W., Barker, N., Martens, A.,
496 Hofhuis, F., DeKoter, R. P., Peters, P. J., Nieuwenhuis, E., & Clevers, H. (2012). Peyer’s Patch
497 M Cells Derived from Lgr5+ Stem Cells Require SpiB and Are Induced by RankL in Cultured
498 “Miniguts.” *Molecular and Cellular Biology*, 32(18), 3639–3647.
499 <https://doi.org/10.1128/mcb.00434-12>
- 500 Giguère, V. (2002). To ERR in the estrogen pathway. In *Trends in Endocrinology and Metabolism*
501 (Vol. 13, Issue 5, pp. 220–225). Elsevier Current Trends. [https://doi.org/10.1016/S1043-](https://doi.org/10.1016/S1043-2760(02)00592-1)
502 [2760\(02\)00592-1](https://doi.org/10.1016/S1043-2760(02)00592-1)
- 503 Hase, K., Kawano, K., Nochi, T., Pontes, G. S., Fukuda, S., Ebisawa, M., Kadokura, K., Tobe, T.,
504 Fujimura, Y., Kawano, S., Yabashi, A., Waguri, S., Nakato, G., Kimura, S., Murakami, T.,
505 Imura, M., Hamura, K., Fukuoka, S. I., Lowe, A. W., ... Ohno, H. (2009). Uptake through
506 glycoprotein 2 of FimH + bacteria by M cells initiates mucosal immune response. *Nature*,
507 462(7270), 226–230. <https://doi.org/10.1038/nature08529>
- 508 Kaikkonen, M. U., Niskanen, H., Romanoski, C. E., Kansanen, E., Kivelä, A. M., Laitalainen, J.,
509 Heinz, S., Benner, C., Glass, C. K., & Ylä-Herttuala, S. (2014). Control of VEGF-A
510 transcriptional programs by pausing and genomic compartmentalization. *Nucleic Acids*
511 *Research*, 42(20), 12570–12584. <https://doi.org/10.1093/nar/gku1036>
- 512 Kamachi, Y., Cheah, K. S. E., & Kondoh, H. (1999). Mechanism of Regulatory Target Selection by
513 the SOX High-Mobility-Group Domain Proteins as Revealed by Comparison of SOX1/2/3 and
514 SOX9. *Molecular and Cellular Biology*, 19(1), 107–120. <https://doi.org/10.1128/mcb.19.1.107>
- 515 Kanaya, T., Hase, K., Takahashi, D., Fukuda, S., Hoshino, K., Sasaki, I., Hemmi, H., Knoop, K. A.,
516 Kumar, N., Sato, M., Katsuno, T., Yokosuka, O., Toyooka, K., Nakai, K., Sakamoto, A.,
517 Kitahara, Y., Jinnohara, T., Mcsorley, S. J., Kaisho, T., ... Ohno, H. (2012). The Ets transcription
518 factor Spi-B is essential for the differentiation of intestinal microfold cells. *Nature Immunology*,
519 13(8), 729–736. <https://doi.org/10.1038/ni.2352>
- 520 Kanaya, T., & Ohno, H. (2014). The Mechanisms of M-cell Differentiation. *Biosci Microbiota Food*
521 *Health*, 33(3), 91-97. <https://doi.org/10.12938/bmfh.33.91>
- 522 Kanaya, T., Sakakibara, S., Jinnohara, T., Hachisuka, M., Tachibana, N., Hidano, S., Kobayashi, T.,
523 Kimura, S., Iwanaga, T., Nakagawa, T., Katsuno, T., Kato, N., Akiyama, T., Sato, T., Williams,

- 524 I. R., & Ohno, H. (2018). Development of intestinal M cells and follicle-associated epithelium
525 is regulated by TRAF6-mediated NF- κ B signaling. *Journal of Experimental Medicine*, 215(2),
526 501–519. <https://doi.org/10.1084/jem.20160659>
- 527 Kim, D. K., Jeong, J. H., Lee, J. M., Kim, K. S., Park, S. H., Kim, Y. D., Koh, M., Shin, M., Jung, Y.
528 S., Kim, H. S., Lee, T. H., Oh, B. C., Kim, J. Il, Park, H. T., Jeong, W. Il, Lee, C. H., Park, S.
529 B., Min, J. J., Jung, S. I., ... Choi, H. S. (2014). Inverse agonist of estrogen-related receptor γ
530 controls *Salmonella typhimurium* infection by modulating host iron homeostasis. *Nature*
531 *Medicine*, 20(4), 419–424. <https://doi.org/10.1038/nm.3483>
- 532 Kim, T. H., Li, F., Ferreiro-Neira, I., Ho, L. L., Luyten, A., Nalapareddy, K., Long, H., Verzi, M., &
533 Shivdasani, R. A. (2014). Broadly permissive intestinal chromatin underlies lateral inhibition
534 and cell plasticity. *Nature*, 506(7489), 511–515. <https://doi.org/10.1038/nature12903>
- 535 Kimura, S., Kobayashi, N., Nakamura, Y., Kanaya, T., Takahashi, D., Fujiki, R., Mutoh, M., Obata,
536 Y., Iwanaga, T., Nakagawa, T., Kato, N., Sato, S., Kaisho, T., Ohno, H., & Hase, K. (2019).
537 *Sox8 is essential for M cell maturation to accelerate IgA response at the early stage after*
538 *weaning in mice*. <https://doi.org/10.1084/jem.20181604>
- 539 Kimura, S., Nakamura, Y., Kobayashi, N., Shioguchi, K., Kawakami, E., Mutoh, M., Takahashi-
540 Iwanaga, H., Yamada, T., Hisamoto, M., Nakamura, M., Udagawa, N., Sato, S., Kaisho, T.,
541 Iwanaga, T., & Hase, K. (n.d.). *Osteoprotegerin-dependent M cell self-regulation balances gut*
542 *infection and immunity*. <https://doi.org/10.1038/s41467-019-13883-y>
- 543 Kishikawa, S., Sato, S., Kaneto, S., Uchino, S., Kohsaka, S., Nakamura, S., & Kiyono, H. (2017).
544 ARTICLE Allograft inflammatory factor 1 is a regulator of transcytosis in M cells. *Nature*
545 *Communications*. <https://doi.org/10.1038/ncomms14509>
- 546 Kishore, N., Sommers, C., Mathialagan, S., Guzova, J., Yao, M., Hauser, S., Huynh, K., Bonar, S.,
547 Mielke, C., Lee, A. ¶, Weier, R., Graneto, M., Hanau, C., Perry, T., & Tripp, C. S. (2003). *A*
548 *Selective IKK-2 Inhibitor Blocks NF-B-dependent Gene Expression in Interleukin-1-stimulated*
549 *Synovial Fibroblasts**. <https://doi.org/10.1074/jbc.M211439200>
- 550 Knoop, K. A., Kumar, N., Butler, B. R., Sakthivel, S. K., Taylor, R. T., Nochi, T., Akiba, H., Yagita,
551 H., Kiyono, H., & Williams, I. R. (2009). RANKL Is Necessary and Sufficient to Initiate
552 Development of Antigen-Sampling M Cells in the Intestinal Epithelium. *The Journal of*
553 *Immunology*, 183(9), 5738–5747. <https://doi.org/10.4049/jimmunol.0901563>
- 554 Kraehenbuhl, J. P., & Neutra, M. R. (2000). Epithelial M cells: Differentiation and function. In
555 *Annual Review of Cell and Developmental Biology* (Vol. 16, pp. 301–332). Annual Reviews
556 4139 El Camino Way, P.O. Box 10139, Palo Alto, CA 94303-0139, USA .
557 <https://doi.org/10.1146/annurev.cellbio.16.1.301>
- 558 Kunimura, K., Sakata, D., Tun, X., Uruno, T., Ushijima, M., Katakai, T., Shiraishi, A., Aihara, R.,
559 Kamikaseda, Y., Matsubara, K., Kanegane, H., Sawa, S., Eberl, G., Ohga, S., Yoshikai, Y., &
560 Fukui, Y. (2019). S100A4 Protein Is Essential for the Development of Mature Microfold Cells
561 in Peyer's Patches. *Cell Reports*, 29(9), 2823-2834.e7.
562 <https://doi.org/10.1016/j.celrep.2019.10.091>
- 563 Lee, T. I., Jenner, R. G., Boyer, L. A., Guenther, M. G., Levine, S. S., Kumar, R. M., Chevalier, B.,
564 Johnstone, S. E., Cole, M. F., Isono, K. ichi, Koseki, H., Fuchikami, T., Abe, K., Murray, H. L.,

- 565 Zucker, J. P., Yuan, B., Bell, G. W., Herbolsheimer, E., Hannett, N. M., ... Young, R. A. (2006).
566 Control of Developmental Regulators by Polycomb in Human Embryonic Stem Cells. *Cell*,
567 *125*(2), 301–313. <https://doi.org/10.1016/j.cell.2006.02.043>
- 568 Mabbott, N. A., Donaldson, D. S., Ohno, H., Williams, I. R., & Mahajan, A. (2013). Microfold (M)
569 cells: Important immunosurveillance posts in the intestinal epithelium. In *Mucosal Immunology*
570 (Vol. 6, Issue 4, pp. 666–677). Nature Publishing Group. <https://doi.org/10.1038/mi.2013.30>
- 571 Mäntylä, E., Salokas, K., Oittinen, M., Aho, V., Mäntysaari, P., Palmujoki, L., Kalliolinna, O.,
572 Ihalainen, T. O., Niskanen, E. A., Timonen, J., Viiri, K., & Vihinen-Ranta, M. (2016). Promoter-
573 Targeted Histone Acetylation of Chromatinized Parvoviral Genome Is Essential for the Progress
574 of Infection. *Journal of Virology*, *90*(8), 4059–4066. <https://doi.org/10.1128/jvi.03160-15>
- 575 Matsushima, A., Kakuta, Y., Teramoto, T., Koshihara, T., Liu, X., Okada, H., Tokunaga, T., Kawabata,
576 S. I., Kimura, M., & Shimohigashi, Y. (2007). Structural evidence for endocrine disruptor
577 bisphenol A binding to human nuclear receptor ERR γ . *Journal of Biochemistry*, *142*(4), 517–
578 524. <https://doi.org/10.1093/jb/mvm158>
- 579 Nagashima, K., Sawa, S., Nitta, T., Tsutsumi, M., Okamura, T., Penninger, J. M., Nakashima, T., &
580 Takayanagi, H. (2017). Identification of subepithelial mesenchymal cells that induce IgA and
581 diversify gut microbiota. *Nature Immunology*, *18*(6), 675–682. <https://doi.org/10.1038/ni.3732>
- 582 Neutra, M. R., Frey, A., & Kraehenbuhl, J. P. (1996). Epithelial M cells: Gateways for mucosal
583 infection and immunization. In *Cell* (Vol. 86, Issue 3, pp. 345–348). Cell Press.
584 [https://doi.org/10.1016/S0092-8674\(00\)80106-3](https://doi.org/10.1016/S0092-8674(00)80106-3)
- 585 Neutra, M. R., Mantis, N. J., & Kraehenbuhl, J. P. (2001). Collaboration of epithelial cells with
586 organized mucosal lymphoid tissues. In *Nature Immunology* (Vol. 2, Issue 11, pp. 1004–1009).
587 Nat Immunol. <https://doi.org/10.1038/ni1101-1004>
- 588 Oittinen, M., Popp, A., Kurppa, K., Lindfors, K., Mäki, M., Kaikkonen, M. U., & Viiri, K. (2017).
589 Polycomb Repressive Complex 2 Enacts Wnt Signaling in Intestinal Homeostasis and
590 Contributes to the Instigation of Stemness in Diseases Entailing Epithelial Hyperplasia or
591 Neoplasia. *STEM CELLS*, *35*(2), 445–457. <https://doi.org/10.1002/stem.2479>
- 592 Owen, R. L. (1999). Uptake and transport of intestinal macromolecules and microorganisms by M
593 cells in Peyer's patches: A personal and historical perspective. *Seminars in Immunology*, *11*(3),
594 157–163. <https://doi.org/10.1006/smim.1999.0171>
- 595 Ram, O., Goren, A., Amit, I., Shoshitaishvili, N., Yosef, N., Ernst, J., Kellis, M., Gymrek, M., Issner, R.,
596 Coyne, M., Durham, T., Zhang, X., Donaghey, J., Epstein, C. B., Regev, A., & Bernstein, B. E.
597 (2011). Combinatorial patterning of chromatin regulators uncovered by genome-wide location
598 analysis in human cells. *Cell*, *147*(7), 1628–1639. <https://doi.org/10.1016/j.cell.2011.09.057>
- 599 Rios, D., Wood, M. B., Li, J., Chassaing, B., Gewirtz, A. T., & Williams, I. R. (2016). Antigen
600 sampling by intestinal M cells is the principal pathway initiating mucosal IgA production to
601 commensal enteric bacteria. *Mucosal Immunology*, *9*(4), 907–916.
602 <https://doi.org/10.1038/mi.2015.121>
- 603 Sato, S., Kaneto, S., Shibata, N., Takahashi, Y., Okura, H., Yuki, Y., Kunisawa, J., & Kiyono, H.
604 (2013). Transcription factor Spi-B-dependent and -independent pathways for the

- 605 development of Peyer's patch M cells. *Mucosal Immunology*.
606 <https://doi.org/10.1038/mi.2012.122>
- 607 Schuettengruber, B., & Cavalli, G. (2009). Recruitment of Polycomb group complexes and their role
608 in the dynamic regulation of cell fate choice. In *Development* (Vol. 136, Issue 21, pp. 3531–
609 3542). The Company of Biologists Ltd. <https://doi.org/10.1242/dev.033902>
- 610 Vizán, P., Beringer, M., & Di Croce, L. (2016). Polycomb-dependent control of cell fate in adult
611 tissue. *The EMBO Journal*, 35(21), 2268–2269. <https://doi.org/10.15252/embj.201695694>
- 612 Walsh, M. C., Choi, Y., Hong, J., & Teitelbaum, S. L. (2014). *Biology of the RANKL-RANK-OPG*
613 *system in immunity, bone, and beyond*. <https://doi.org/10.3389/fimmu.2014.00511>
- 614 Wang, L., Jin, Q., Lee, J. E., Su, I. H., & Ge, K. (2010). Histone H3K27 methyltransferase Ezh2
615 represses Wnt genes to facilitate adipogenesis. *Proceedings of the National Academy of Sciences*
616 *of the United States of America*, 107(16), 7317–7322. <https://doi.org/10.1073/pnas.1000031107>
- 617 Yilmaz, Z. B., Weih, D. S., Sivakumar, V., & Weih, F. (2003). RelB is required for Peyer's patch
618 development: Differential regulation of p52-RelB by lymphotoxin and TNF. *EMBO Journal*,
619 22(1), 121–130. <https://doi.org/10.1093/emboj/cdg004>
- 620 Zuercher, W. J., Gaillard, S., Orband-Miller, L. A., Chao, E. Y. H., Shearer, B. G., Jones, D. G.,
621 Miller, A. B., Collins, J. L., McDonnell, D. P., & Willson, T. M. (2005). Identification and
622 structure-activity relationship of phenolic acyl hydrazones as selective agonists for the estrogen-
623 related orphan nuclear receptors ERR β and ERR γ . *Journal of Medicinal Chemistry*, 48(9), 3107–
624 3109. <https://doi.org/10.1021/jm050161j>

625

626

627 **Figure legends**

628

629 **Figure 1. PRC2 members are expressed in M cells.** A) RT-qPCR analyses of the expression of
630 Suz12 and Ezh2 in mouse intestinal organoids grown in ENR, ENR+RankL and ENRI conditions. B)
631 Immunoblot of H3K27me3 and H3 in organoids treated with E11 inhibitor. Data are representative of
632 2 independent experiments. C) RT-qPCR analyses of the expression of M cell marker genes in
633 RankL-treated organoids with or without EZH2 inhibitor E11. Unpaired two-tailed Student's *t* test
634 was performed, n.s., not significant; *, $P < 0.05$; **, $P < 0.01$; ***, $P < 0.005$, $n = 3$. Values are
635 presented as the mean \pm SD

636 **Figure 2. PRC2 regulated genes during the M cell differentiation.** A) Differentially expressed
637 genes during M cell differentiation detected with Gro-Seq. Signal is depicted by volcano plot
638 comparing organoids before and after RankL treatment. X-axis and Y-axis indicate the log₂ fold
639 change and $-\log_{10}$ adjusted P-value. Differentially expressed genes are marked (Gro-Seq with log₂
640 fold change cutoff at ± 2 and P -value < 0.0001). Upregulated genes from ENRI conditions were
641 removed to show only RankL specific regulation. B) Genes upregulated in M cells compared to stem
642 cells and enterocytes. Heatmap of differentially expressed (Gro-Seq with log₂ fc cutoff at ± 2 and
643 P -value < 0.0001) and H3K27me3 regulated (log₂ fc ± 2 , P -value $< 10^{-6}$) genes in RankL, ENRI and

644 WENRC treated organoids showing centered log₂ fold change. C) Genes downregulated by
645 H3K27me₃ in M cells and enterocytes compared to stem cells. D) Genes downregulated by
646 H3K27me₃ in stem cells and M cells compared to enterocytes. E) Composite enrichment analysis of
647 H3K27me₃ signal density +4000 bases around transcription start sites in genes specifically silenced
648 by PRC2 in M cells (above) and specifically expressed in M cells (below). F) Gene ontologies
649 enriched ($P < 0.05$) in differentially expressed PRC2-target genes between M cells and stem cells
650 (GRO-Seq log₂ fc +2, P-value <0.0001 and H3K27me₃ log₂ fc +2, P-value < 10⁻⁶) in molecular
651 function and biological process.

652 **Figure 3. Esrrg is expressed in FAE in Peyer's patches and is dependent on Rank-RankL**
653 **signalling.** A) H3K27me₃ occupancy at CpG islands spanning the promoter and first exon of the
654 Esrrg gene in organoids treated with RankL (M cells) or inhibited with IWP2 (Enterocytes) or treated
655 with Wnt3a and Chir99021 (Crypt/ISCs). Below, pre-mRNA expression of Esrrg in organoids treated
656 as above (y-axis: normalized tag count, ENR500 = R-spondin 500ng/ml, R100 = Rankl 100ng/ml).
657 B) Section of PP from wild-type mice stained with Esrrg antibody. Arrowheads indicating Esrrg
658 expression in the nuclei of M cells in FAE. C) RT-qPCR analysis of Esrrg and Gp2 in the FAE and
659 VE from C57BL/6JRj mice ($n = 3$ from wild-type mice). D) Organoids generated from wild-type
660 mice were stimulated with 100ng of RankL for 4 d. Esrrg and Gp2 expression was examined by
661 quantitative PCR analysis. E) Rank KO organoids and Scrambled organoids generated by
662 lentiCRISPR v2 were incubated with RankL for 4 days, Esrrg and GP2 expression was analyzed by
663 quantitative RT-qPCR. In (C-E) unpaired two-tailed Student's *t* test was performed for three
664 independent experiments, ****, $P < 0.0005$; ***, $P < 0.005$; **, $P < 0.01$.

665

666

667 **Figure 4. Esrrg expression is induced by RelB/p52 activation.** A) Lta1β2 prominently upregulated
668 the expression of Esrrg in organoids. Organoids from C57BL/6JRj mice were stimulated with LTα1β2
669 for 3 d, and the gene expression was analyzed by quantitative PCR. B) Organoids from wild-type
670 mice were stimulated with RankL for 3 d in the absence or presence of 125μM SC-514. Gene
671 expression was analyzed by quantitative PCR. C) Organoids were transduced to express classical and
672 non-canonical NF-κβ and the expression of Esrrg and Spi-B (control) are represented in relative to
673 Gapdh D) Organoids expressing p52 and RelB in the presence of SC-514 for 3 d, and the expression
674 of Esrrg and Spi-B was analyzed by quantitative PCR. Values in all are presented as the mean ± SD
675 and unpaired two-tailed Student's *t* test was performed, $n=3$; n.s, not significant; **, $P < 0.01$; ***, P
676 < 0.005 .

677

678 **Figure 5. Abolition of Esrrg impairs Sox8 activation and the functional maturation of M cells.**
679 A) Schematic representation of Esrrg knockout design by CRISPR-Cas9 genome editing in mouse
680 intestinal organoids. Exon, intron, and genomic position are indicated. B) Esrrg protein expression in
681 Esrrg KO and Scrambled cells generated by lentiCRISPR v2 genome editing in C57BL/6JRj intestinal
682 organoids. Organoid lysates were analyzed by Western blot. C) qPCR analysis of M cell associated
683 genes expressed in in vitro culture stimulated by RankL for 4 days. D) Immunostaining images for
684 Spi-B (red), Sox8 (red) and Gp2 (green) in Scrambled organoids with and without RankL 100ng for
685 4 days and Esrrg KO with and without RankL 100ng, Bars, 100 μm. E) qPCR analysis of early
686 markers of M cell associated genes expressed in vitro in the presence of RankL for 4 days. Values in

687 all are presented as the mean \pm SD. Unpaired two-tailed Student's t test, n=3, ns, not significant; **,
688 P < 0.01; ****, P < 0.0005.

689 **Figure 6. Esrrg expression and its relation to other M Cell developmental markers Spi-B and**
690 **Sox8** A) Esrrg expression was unaffected by lack of Sox8 expression. qPCR analysis of Esrrg and
691 Gp2 in the FAE and VE from Sox8^{+/+} and Sox8^{-/-} mice. B) Organoids generated from Sox8^{+/+} and
692 Sox8^{-/-} mice were stimulated with and without RankL for 4 d. Esrrg expression was examined by
693 quantitative PCR analysis. C) Organoids isolated from Sox8 wild-type and Sox8 KO mice were lysed
694 and analyzed by Western blot for Esrrg expression. D) qPCR analysis of Esrrg in a Spi-B knockout
695 intestinal organoids by lentiCRISPR v2. E) Organoid lysates for Esrrg in Scrambled and SpiB KO
696 organoids were analyzed by Western blot. Values in all are presented as the mean \pm SD. Unpaired
697 two-tailed Student's t test, n=3, ns, not significant; *, P<0.05; **, P < 0.01.

698

699 **Figure 7. Esrrg alone is not sufficient for maturation of GP2+ M cells.** A) Intestinal organoids
700 were dissociated and transduced by lentivirus encoding Esrrg. qPCR analysis of Spi-B, Sox8 and GP2
701 showed no significant changes. B) Organoids were grown in the presence and absence of 100ng/ml
702 Rankl and 1 μ m of tamoxifen-antagonist of Esrrg. Spi-B, Gp2 and Sox8 expression was analyzed with
703 RT-qPCR. C) Intestinal organoids from mouse were grown in the presence and absence of Rankl
704 100ng/ml and 10 μ m GSK 4718- agonist of Esrrg for 3 days. Spi-B, Gp2 and Sox8 analyzed with RT-
705 qPCR. Values are presented as the mean \pm SD. Unpaired two-tailed Student's t test, n =3. n.s., not
706 significant. *, P < 0.05; **, P < 0.01; ****, P < 0.005.

707 **Figure 8. PRC2 regulates the differentiation of M-cell.** In the absence of Rank-RankL signaling,
708 Esrrg and Sox8 genes are repressed by PRC2 in the intestinal epithelium. When migrating progenitors
709 with Rank receptors binds to RankL in Peyer's patches, this induces NF- κ B signaling leading to loss
710 of H3K27me3 from the gene promoters and activation of Esrrg and Sox8. Sustained expression of
711 Sox8 and GP2 and differentiation of M cells is dependent on Esrrg.

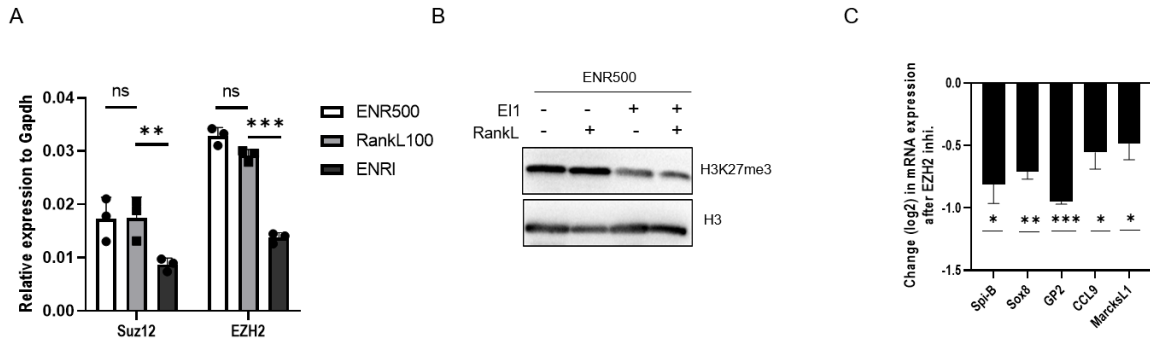
712

713 **Supplementary table 1.** Gro-seq data for the organoids treated with Rankl and compared to
714 organoids grown in enterocyte differentiation (ENRI) and and stemness (WENRC) conditions.

715

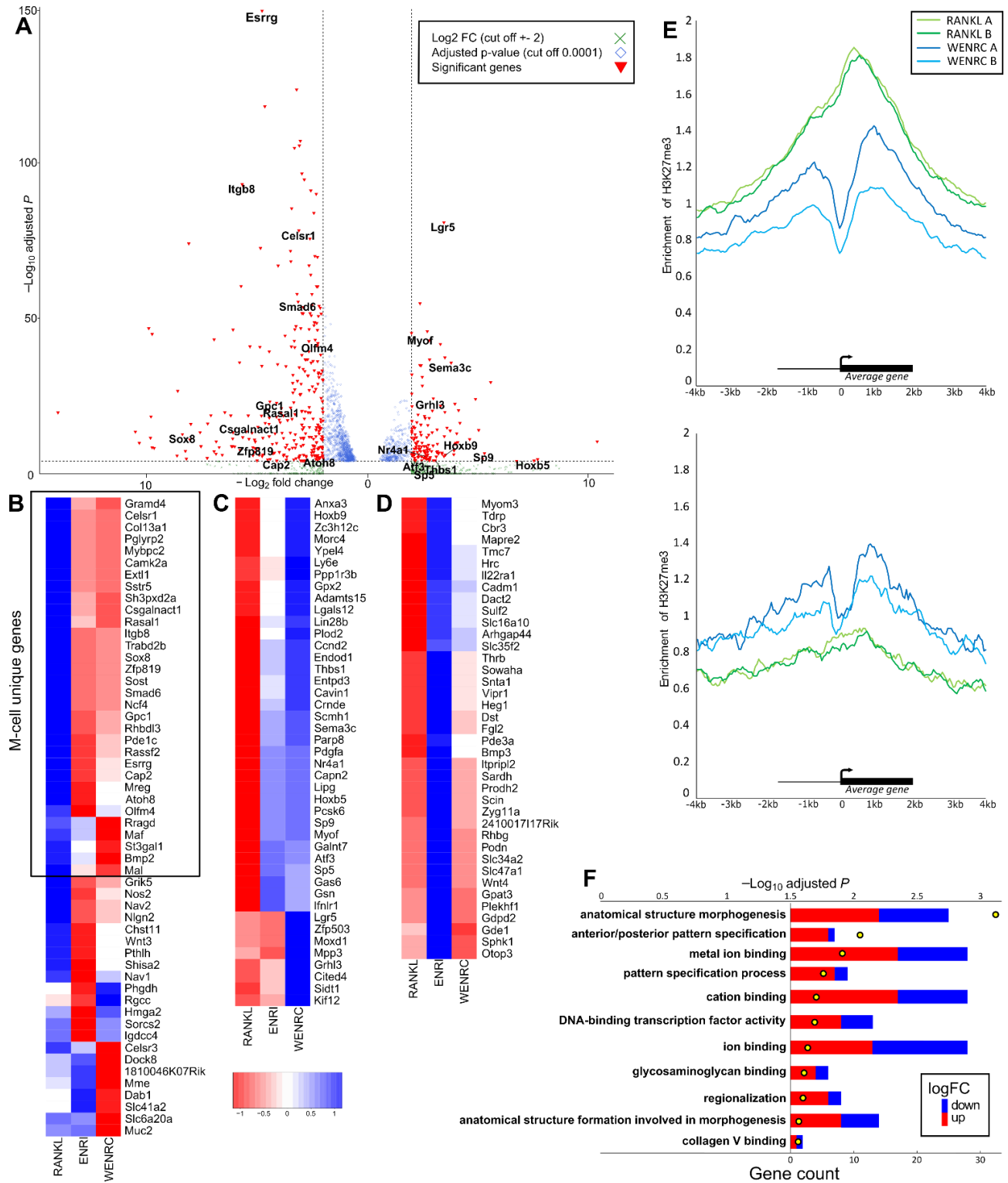
716 **Supplementary table 2.** H3K27me3 ChIP-seq data for the organoids treated with Rankl and grown
717 in stemness condition (WENRC)

718



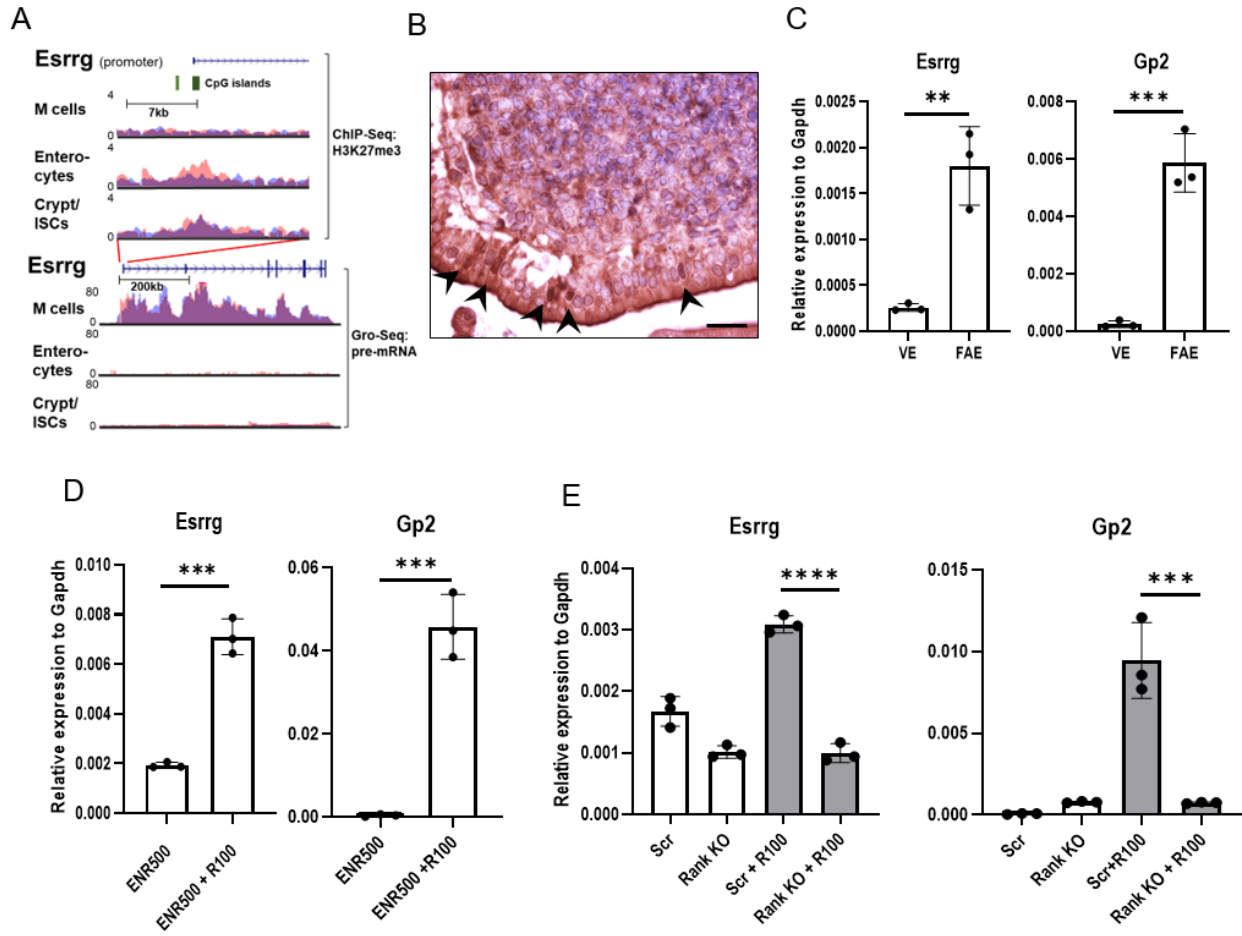
719

720 **Figure 1.**



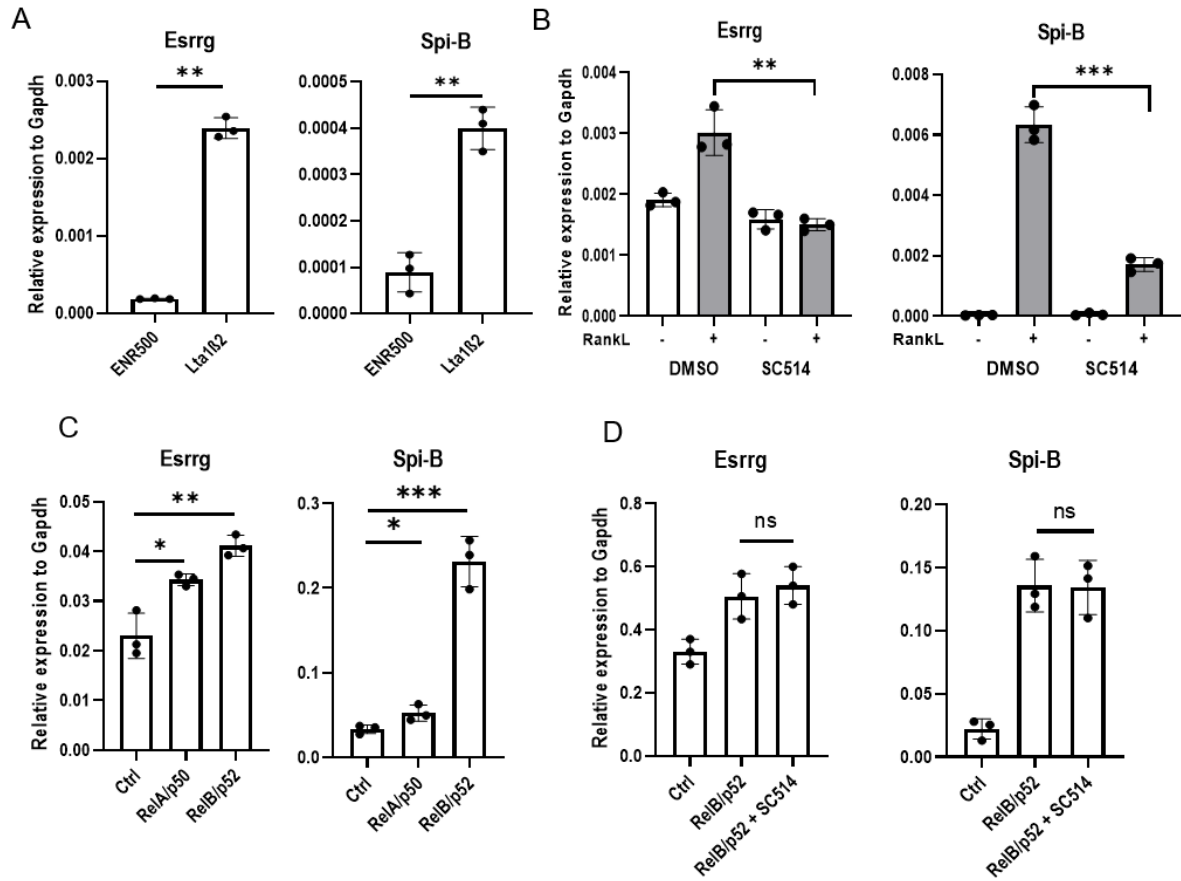
721

722 **Figure 2.**



723

724 **Figure 3.**



725

726

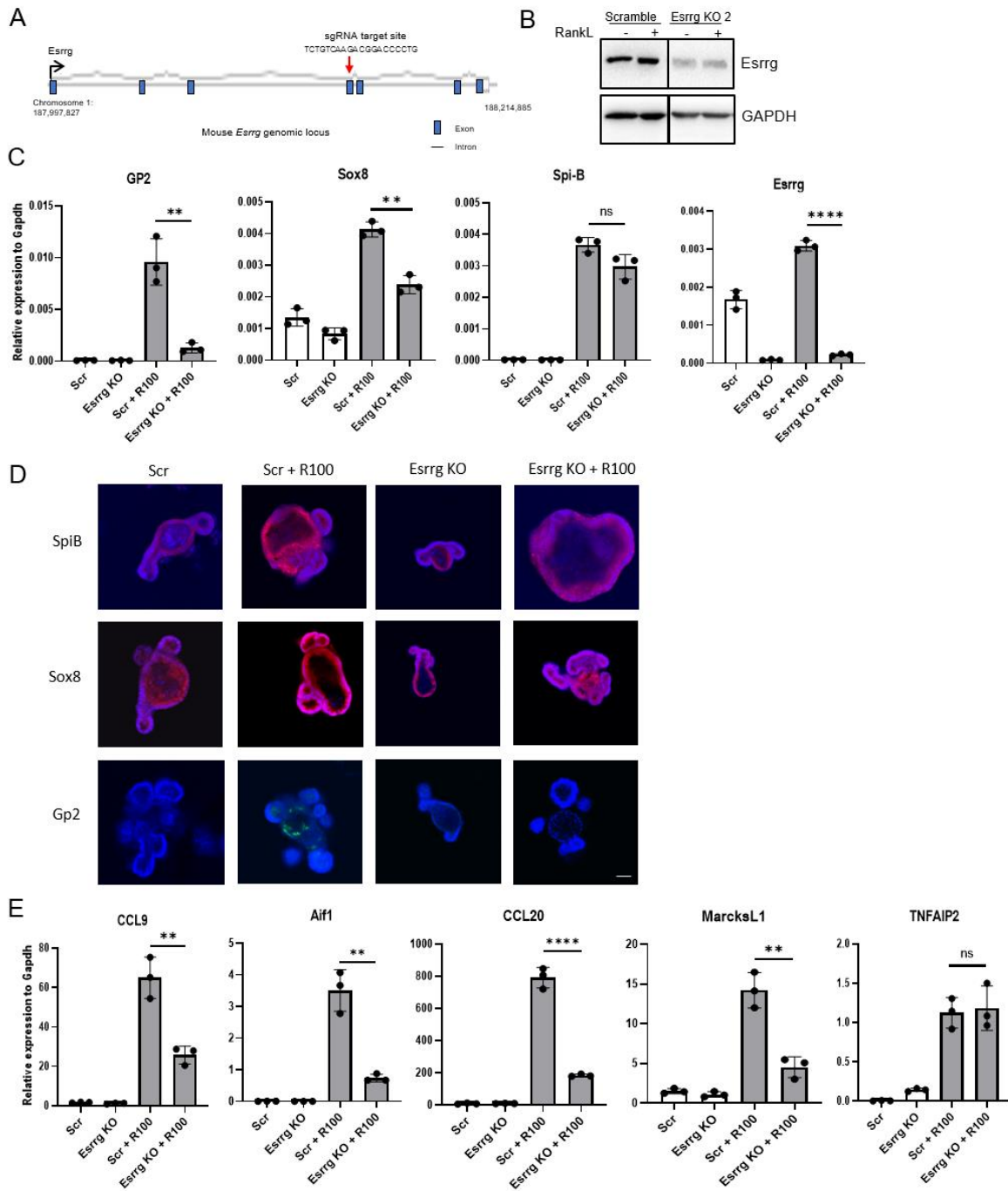
727 **Figure 4.**

728

729

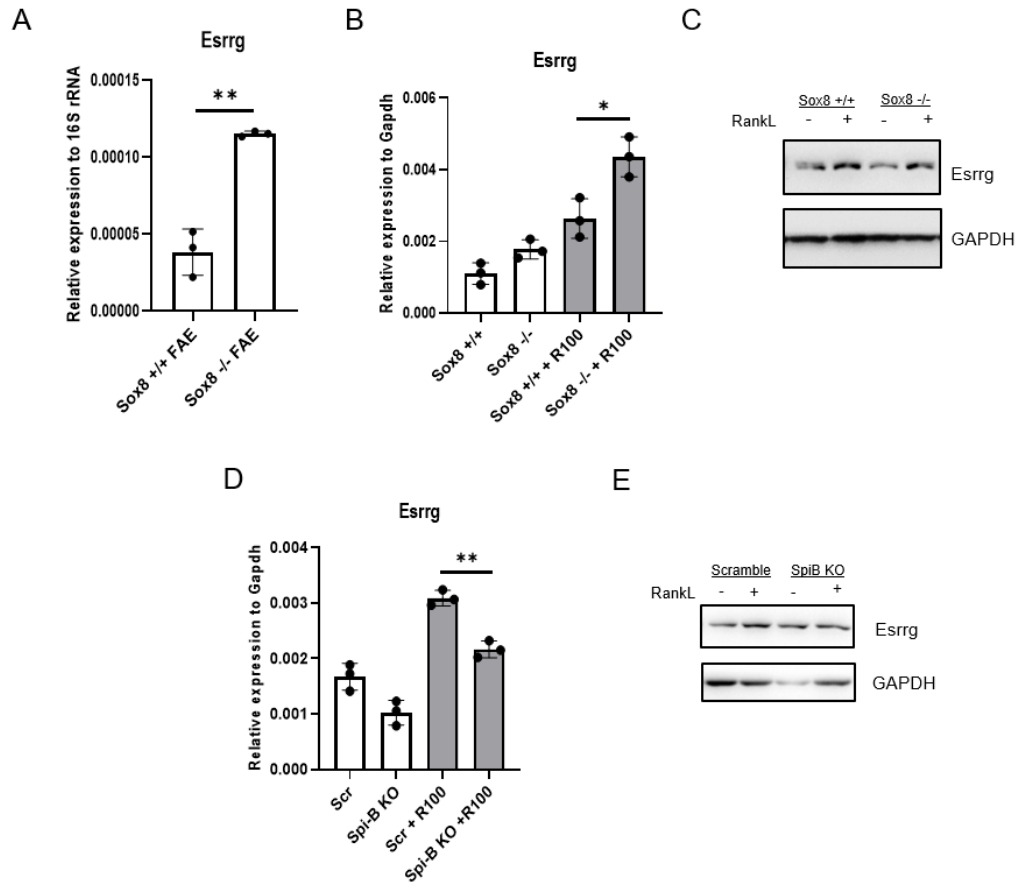
730

731



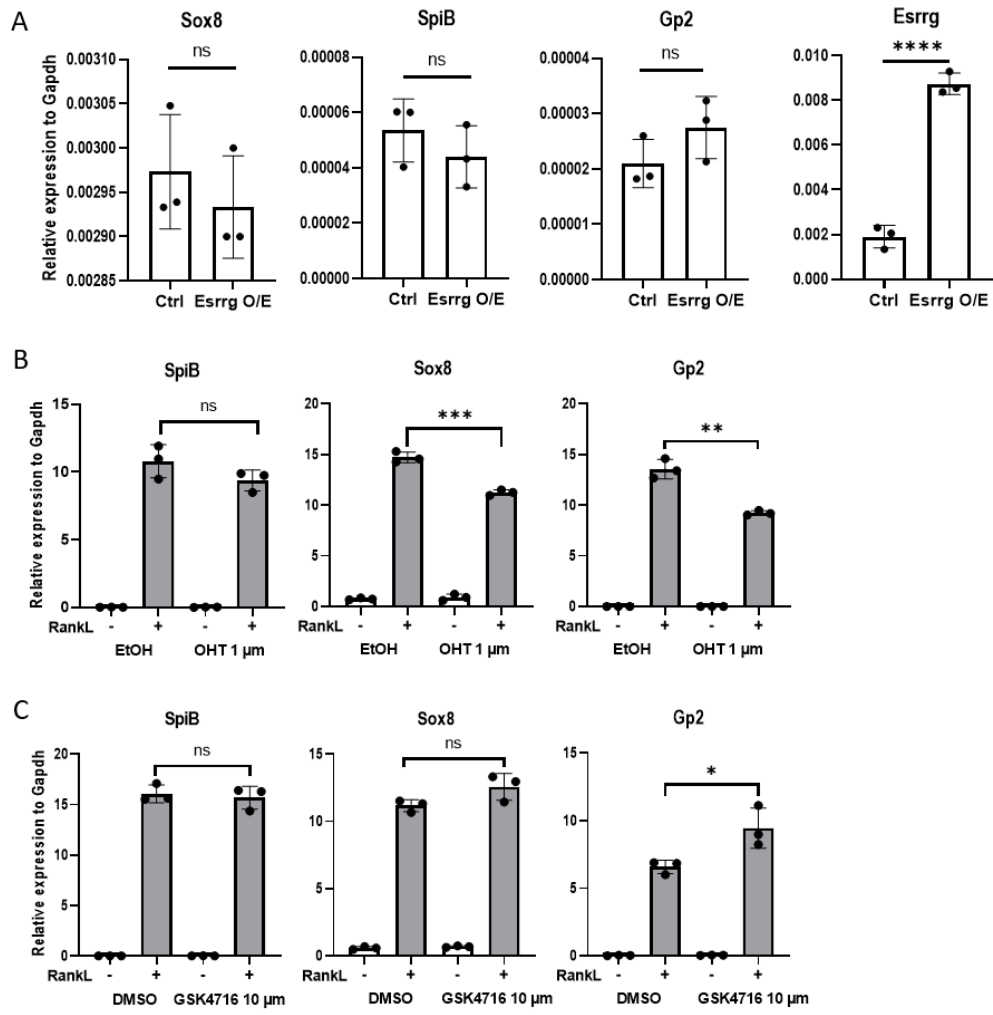
732

733 **Figure 5.**



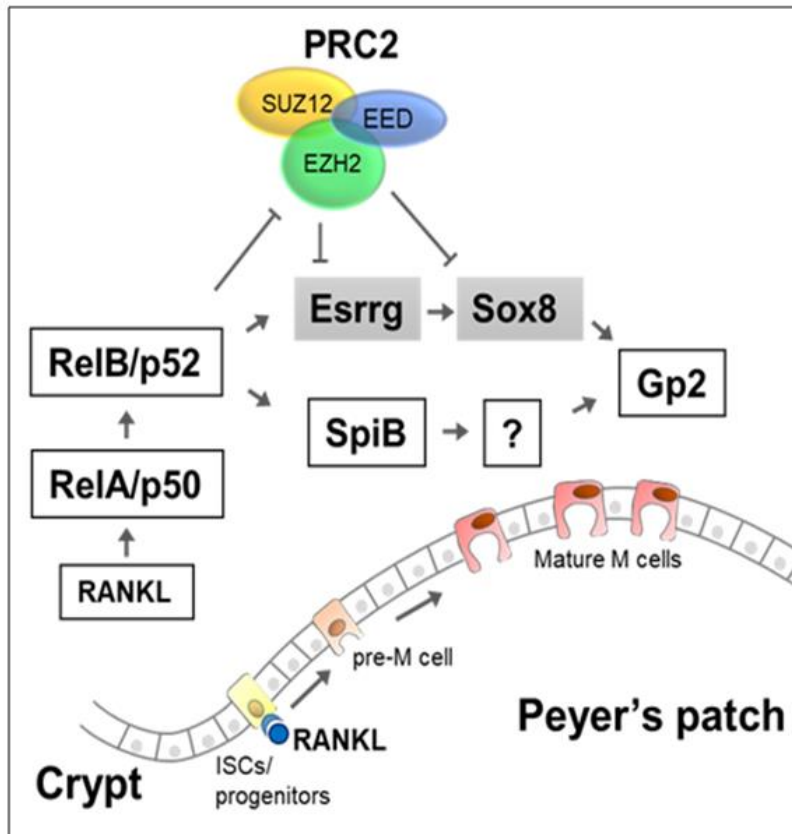
734

735 **Figure 6.**



736

737 **Figure 7.**



738

739 **Figure 8.**

740